ACS OMEGA

http://pubs.acs.org/journal/acsodf

Article

Chiral Self-Sorting and the Realization of Ferroelectricity in the Columnar Liquid Crystal Phase of an Optically Inactive *N,N′*-Diphenylurea Derivative Possessing Six (±)-Citronellyl Groups

Miyu Moriya, Michinari Kohri, and Keiki Kishikawa*

Cite This: *ACS Omega* 2021, 6, 18451−18457

Read Online

ACCESS | Metrics & More | Article Recommendations | Supporting Information

ABSTRACT: An axially polar-ferroelectric columnar liquid crystal (AP-FCLC) phase that exhibits both switching and maintenance of the macro-polarity in the column axis direction has been achieved in an *N,N′*-bis(3,4,5-trialkoxyphenyl)urea compound (*rac*-**1**) prepared from (±)-citronellyl bromide. Although it had been thought that chirality is necessary to achieve the AP-FCLC phase from our previous study, the optically inactive compound which is a mixture of 21 stereoisomers, generated an AP-FCLC phase. We confirmed its ferroelectricity and investigated the mechanism for realizing the AP-FCLC phase using optoelectronic experiments, X-ray diffraction, and circular dichroism spectroscopy. As a result, it was suggested that chiral self-sorting occurs in the columnar liquid crystal phase, in which molecules with a similar stereochemistry form a one-handed helical column, and columns with the same helicity gather together to form a chiral domain. Accordingly, we conclude that the optically inactive compound *rac*-**1** also indicates ferroelectricity similar to that of an optically pure urea compound because of chiral self-sorting.

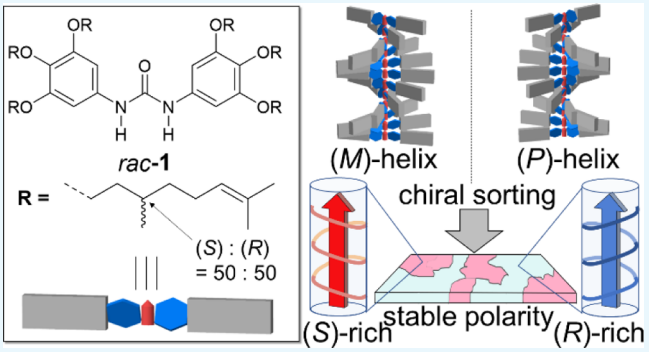

INTRODUCTION

Recently, axially polar ferroelectric columnar liquid crystal (AP-FCLC) phases (Figure 1), in which the polarity along the column axis is induced by applying an electric field and is maintained after removal of the electric field, have been increasingly studied.[1−7] In the columnar liquid crystal (LC) phase, the polar directions of the molecules (Figure 1a) are fixed to generate a polar column (Figure 1b) by intermolecular steric interactions[8−14] or intermolecular hydrogen bonding between the groups such as amide,[4,15−28] urea,[29−31] triazole,[32] and vinylidene fluoride oligomer (VDFO)[33] groups. The polar columns that are self-organized into a nonpolar state (Figure 1c) are polarized by applying an electric field, and the induced columnar polarities are switched (Figure 1d,e) by changing the directions of the applied electric field. The AP-FCLC phase has the potential to realize writable, rewritable, and nonvolatile nano-sized memory devices if one-bit of information can be recorded by a nano-sized electrode.[2,4,31] However, it is still challenging to maintain the induced polarization after removal of the electric field, and we believe that polarization maintenance is most important to realize nonvolatile memory devices.

In 2012, two examples of time scanning of the residual polarization after removal of the applied voltage were reported. Fitié et al.[34] reported that the directions of the three amide carbonyl groups in benzenetrisamides (BTA) were controlled by an applied electric field in an LC cell with a 5 μm cell gap and that the induced polarization was maintained for a long time (1−1000 s). Miyajima et al. reported an AP-FCLC phase of a benzene derivative, possessing two cyano and two amide groups forming core−shell columnar structures,[4] and indicated that the polarity induced by corona poling was maintained at 80% even after 1000 min.

More recently, it was reported that LC compounds possessing a large coercive electric field (E_c), an electric field necessary for switching, show ferroelectricity by sandwiching a submicron thin sample film between two metal electrodes. FCLCs with a large E_c are advantageous in maintaining the induced polar state because their depolarization processes are suppressed by the large energy barrier. In 2016, Urbanaviciute et al. reported ferroelectricity in LC BTA films (thickness: 350−400 nm),[21,35] and in 2019, Casellas et al. reported ferroelectricity in an LC benzotrithiophenetrisamide (BTTTA) film (thickness: 300−800 nm).[20] These ferroelectric LC C_3 symmetric trisamides require a large E_c (coercive fields of BTA

Received: May 14, 2021
Accepted: June 25, 2021
Published: July 10, 2021

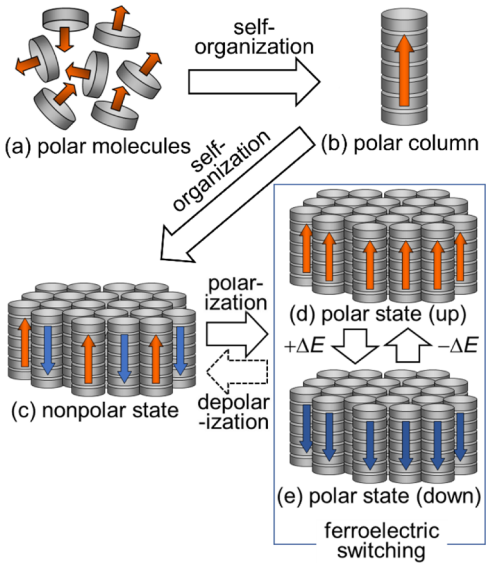

Figure 1. Behaviors of the AP-FCLC phase: (a) polar molecules, (b) polar column, (c) nonpolar state, (d) polar state (upward polarity), and (e) polar state (downward polarity).

and BTTTA: 25−225 and 150−300 V μm^{-1}). García-Iglesias et al. in 2016[33] and Gorbunov et al. in 2017[36] reported that VDFO-functionalized perylenebisimides and phthalocyanines showed ferroelectricity, and that the E_c values measured in the 1 μm thin films were also large (100 and 25 V μm^{-1}, respectively).

In 2020, our group also reported ferroelectricity in a rather thick layer (5 μm) of a chiral urea compound, *N*,*N*′-bis(3,4,5-tri(*S*)-citronellyloxyphenyl)urea [(*S*)-**1**][31] (Scheme 1), which

Scheme 1. Molecular Structures of *rac*-1, (*S*)-1, (*R*)-1, and Urea-10

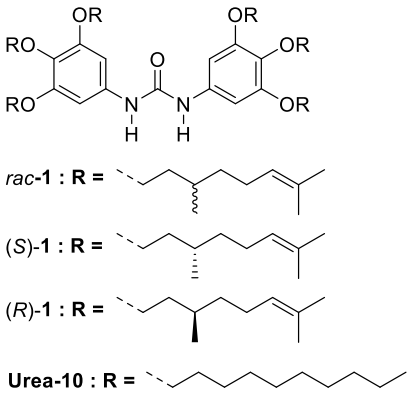

achieved both a low E_c (4.12 V μm^{-1}) and highly stable polarization (the polarity quantitatively remained even after 8 h). From the comparison of (*S*)-**1** with non-chiral ureas [e.g., **Urea-10** (R = $(CH_2)_9CH_3$)],[29,31] we concluded that the helical structure generated by the chirality played an important role in generating its unique ferroelectricity. This result was because the one-handed, tightly wound helix kept the intermolecular distances between the substituent groups short, which effectively strengthened the attractive intermolecular interactions, such as alkyl−alkyl, phenyl−phenyl, and dipole−dipole interactions, in each column.

To verify the effect of chirality on the generation of the FCLC phase of (*S*)-**1**, we prepared urea compound *rac*-**1** from (±)-citronellyl bromide. Since compound *rac*-**1** is optically inactive, it was proposed that *rac*-**1** would not show ferroelectricity. However, surprisingly, the columnar phase of *rac*-**1** shows a perfect ferroelectricity similar to that of (*S*)-**1**, possessing six (*S*)-citronellyl groups. Because either of the (*S*)- or (*R*)-citronellyl groups is introduced to each of its six substituent groups in the *rac*-**1** molecule with the same probability, compound *rac*-**1** should be a mixture of 21 stereoisomers and optically inactive.

In this study, the ferroelectric properties of *rac*-**1** are investigated, and the mechanism for the generation of the ferroelectricity in the columnar LC phase is discussed. As a result, we conclude that the key to the generation of the ferroelectricity of *rac*-**1** is chiral self-sorting in the columnar LC phase.

RESULTS AND DISCUSSION

Synthesis of Diphenylureas 1. Compounds *rac*-**1**, (*S*)-**1**, and (*R*)-**1**, as shown in Scheme 1, were prepared as follows (the synthetic route and procedures are shown in Figure S1 and Supporting Information). Pyrogallol was alkylated with (±)-, (*S*)-, and (*R*)-citronellyl bromide to provide the corresponding 1,2,3-trialkoxybenzenes. Nitration of the trialkoxybenzenes with $NaNO_2/HNO_3$ followed by reduction with iron powder in ethanol/water in the presence of ammonium chloride produced 3,4,5-trialkoxyanilines. The aniline derivatives were reacted with 1,1′-carbonyldiimidazole to produce diphenylureas **1**.

Identification of the Phase Transition Behaviors. The phase transition behaviors (Table 1) were investigated by

Table 1. Phase Transition Temperatures of *rac*-1, (*S*)-1, and (*R*)-1[a]

compound	phase transition behaviors
rac-**1**	$Col_r \underset{149.9(-1.0)}{\overset{152.1(1.1)}{\rightleftharpoons}} Col_h \underset{151.7(-0.9)}{\overset{154.5(0.8)}{\rightleftharpoons}}$ Iso
(*S*)-**1**	$Col_r \underset{143.3(-0.2)}{\overset{145.7(0.3)}{\rightleftharpoons}} Col_h \underset{147.4(-0.7)}{\overset{150.2(0.8)}{\rightleftharpoons}} N_{col} \underset{148.5(-1.0)}{\overset{152.2(1.0)}{\rightleftharpoons}}$ Iso
(*R*)-**1**	$Col_r \underset{142.3(-0.2)}{\overset{143.6(0.2)}{\rightleftharpoons}} Col_h \underset{147.5(-0.7)}{\overset{149.6(0.7)}{\rightleftharpoons}} N_{col} \underset{150.1(-0.9)}{\overset{152.8(1.0)}{\rightleftharpoons}}$ Iso

[a]Col_r: rectangular columnar, Col_h: hexagonal columnar, N_{col}: nematic columnar, and Iso: isotropic phases. The numbers above and below the arrows are the transition temperatures (°C), and the numbers in parentheses are the transition enthalpy changes (kJ mol^{-1}), determined by DSC (temperature rate: 2 °C min^{-1}) on the second heating and cooling cycle. The DSC measurements of these LCs were performed above room temperature, and no melting point was observed in the measurement range.

polarized light optical microscopy (POM). Upon cooling, *rac*-**1** showed an isotropic (Iso) to hexagonal columnar (Col_h) phase transition. As shown in Figure 2a, both planarly and homeotropically aligned domains are observed. Further cooling caused the phase transition from the Col_h phase to the rectangular columnar (Col_r) phase, and the dark texture of the Col_h phase changed to a bright texture (Figure 2b) of the Col_r phase at the transition. No change in the texture of the Col_r phase was observed down to room temperature. Then, the phase transition temperatures were investigated by differential scanning calorimetry (DSC). The *rac*-**1**, (*S*)-**1**, and (*R*)-**1**

https://doi.org/10.1021/acsomega.1c02534
ACS Omega 2021, 6, 18451−18457

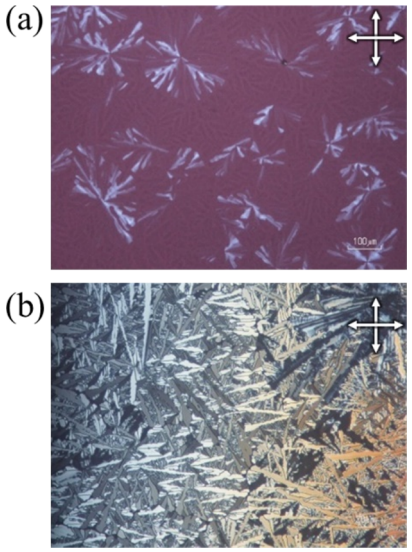

Figure 2. Microphotographs of *rac*-**1** at (a) 151 °C (Col_h phase) and (b) 148 °C (Col_r phase) upon cooling. The arrows indicate the directions of the polarizers.

compounds had a Col_h-Col_r phase transition. In addition, (*S*)-**1**[31] and (*R*)-**1** showed a phase between the Col_h and Iso phases, and this phase was identified to be a nematic columnar (N_{col}) phase by X-ray diffraction (XRD) measurements, although it was not observable in the POM results. A N_{col} phase is a more disordered columnar phase, in which the columns are roughly parallel to each other and there is no long-range order.

Investigation of the Molecular Packing Structure. The molecular packing structure of *rac*-**1** was investigated by XRD. Upon heating, the XRD pattern of *rac*-**1** at 144 °C (Figure 3a) showed *d*(200), *d*(110), *d*(400), *d*(600), and *d*(420) peaks, indicating a Col_r phase (centered lattice) with lattice constants a = 49.6 Å, b = 18.3 Å, c = 4.7 Å, and Z = 2.3. Upon further heating to 154 °C (Figure 3b), only one peak at 20.1 Å was observed. By considering its dendritic texture with sixfold

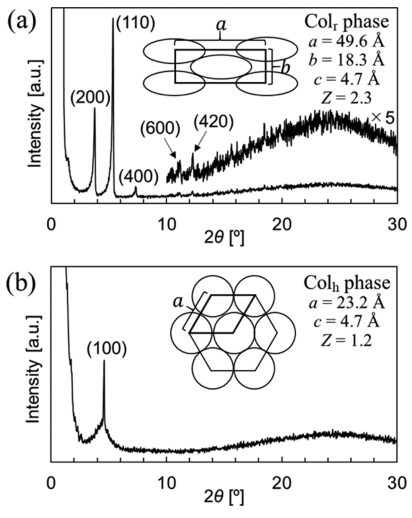

Figure 3. XRD profiles of *rac*-**1** at (a) 144 °C (Col_r phase) and (b) 154 °C (Col_h phase). The lattice constant c (=4.7 Å) reported in our previous study[31] was used. The italic letters *a*, *b*, and c are the lattice parameters. Z indicates the number of molecules in one unit lattice.

symmetry, as shown in Figures 2a and S2, it was assigned to be a Col_h phase (primitive lattice) with lattice constants a = 23.2 Å, c = 4.7 Å, and Z = 1.2. The broad halo at around the *d*(100) peak indicates partially collapsed hexagonal order.

Electro-optical Characterization of *rac*-1. Compound *rac*-**1** was introduced into an indium tin oxide (ITO) glass cell (cell gap: 5 μm, ITO area size: 1 cm × 1 cm, ITO was coated with a polyimide film) by the capillary action in its Iso phase (Figure 4a). Then, a rectangular wave voltage (200 V_{pp} with

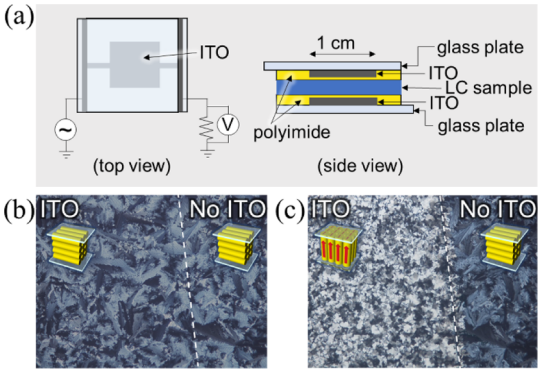

Figure 4. Electro-optic experiment of *rac*-**1** at 144 °C (Col_r phase): (a) experimental apparatus for observing polarity switching (cell gap: 5 μm, ITO area size: 1 cm × 1 cm, ITO was coated with a polyimide film); and microphotographs of the textures (b) before and (c) after applying a rectangular wave voltage for 5 min (frequency: 1.0 Hz, voltage: 200 V_{pp}). The white dashed line is the boundary between the ITO and non-ITO areas.

1.0 Hz) was applied to the sample at 144 °C (Col_r phase), and the texture of the sample on the ITO area immediately changed to a mosaic texture due to the change from a planar to homeotropic alignment (Figure 4b,c).

Investigation of the Macroscopic Polarity of Homeotropically Aligned *rac*-1. To investigate the macroscopic polarity of *rac*-**1** in the Col_r phase, second harmonic generation (SHG) measurement was performed, which is known as an established method to investigate the polarity in materials.[4,37] An overview of the SHG measurement system is shown in Figure 5a,b. By irradiation of an infrared laser beam [Nd:YAG (10 Hz), λ = 1064 nm] to the sample in the LC cell with macroscopic polarity, an SH wave (λ = 532 nm) from the sample is generated. The result of the SHG measurement is shown in Figure 5c. By applying a DC voltage (+100 V_{DC}) for 1 min, the SHG intensity immediately increased. After removal of the voltage, the SHG intensity was maintained even after 6 h. Before applying the voltage, *rac*-**1** showed planar textures in the POM results, indicating that the columns were planarly aligned to the substrate. After applying the voltage, each urea-carbonyl group of *rac*-**1** responded to the voltage, the columns were aligned in parallel to the electric field, and the textures on the ITO area changed to the abovementioned mosaic texture because of the vertical alignment of the columns to the substrate. However, the switching current peak under applying a triangle wave volage (frequency: 1.0 Hz, voltage: 200 V_{pp}) was not detected because the switching response was slow.

Subsequently, the direction of the macroscopic polarization in the sample was investigated by SHG interference experiments. In the SHG interference experiments, a quartz plate is placed next to the laser source to generate a standard SH wave, and a glass plate was set between the quartz plate and the

https://doi.org/10.1021/acsomega.1c02534
ACS Omega 2021, 6, 18451−18457

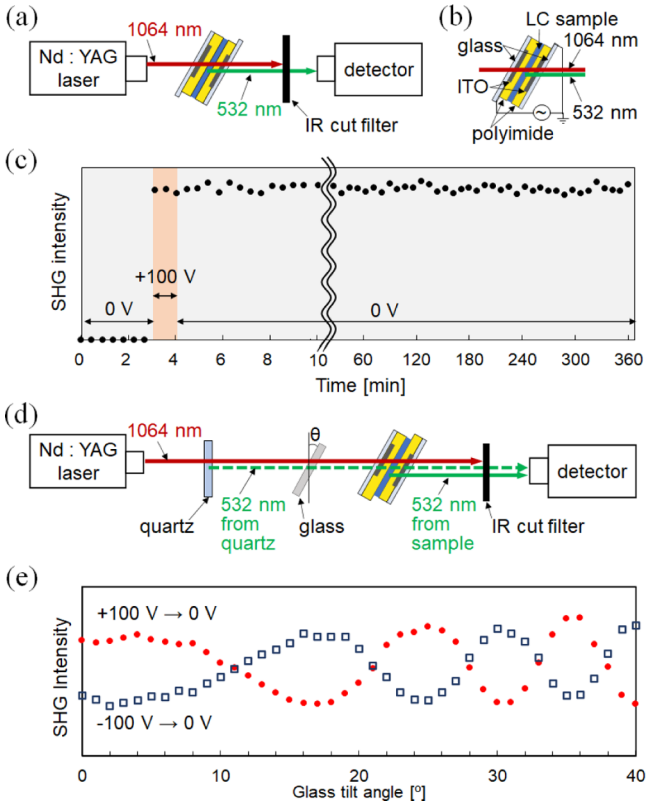

Figure 5. SHG experiments of *rac*-**1**: (a) setup for SHG observation, (b) LC cell with the name of each part, and (c) plots of the SHG intensity of *rac*-**1** at 144 °C (Col_r phase). The voltage was controlled as follows: 0 V (3 min) → +100 V_{DC} (1 min) → 0 V (360 min). (d) Setup for the SHG interferometry observation and (e) plots of SHG intensities of *rac*-**1** at 144 °C (Col_r phase) measured after applying +100 V_{DC} (red filled circle) and −100 V_{DC} (blue open square) for 1 min followed by removal of the voltage.

sample to control the light path length of the laser and SHG lights (Figure 5d). The SH waves from the quartz and the polarized sample interfered with each other. Since the light path lengths of the laser and standard SH lights were changed by rotating the glass plate, plots of the SHG intensity against the glass plate angle formed an interferent curve depending on the polar direction of the sample. At 144 °C (Col_r phase), after applying +100 V_{DC} for 1 min followed by removal of voltage, the SHG intensity was measured with a detector by rotating the glass plate from 0 to 40° (Figure 5e, red filled circle). Then, at this temperature, after −100 V_{DC} application for 1 min followed by removal of the voltage, the SHG intensity was measured using the same procedure (Figure 5e, blue open square). The two obtained interference curves showed line symmetry, which indicated that macroscopic polar directions of the sample in the LC cell were inversed by applying a DC voltage for 1 min.

By these two SHG experiments of *rac*-**1** in the Col_r phase, it was confirmed that the macroscopic polarity induced by applying the voltage was maintained even after removal of the voltage, and the polar direction could be switched by applying an external voltage. Although compound *rac*-**1** is not optically active, it is clear that true ferroelectricity is realized in the Col_r phase.

Furthermore, to investigate the coercive electric field (E_c) of *rac*-**1** in the Col_r phase, the SHG interferometry experiment was performed at 134 °C with setting the glass angle at 0° on applying a triangular voltage (voltage: 100 V_{pp}, frequency: 20 mHz, cell gap: 5 μm), and the SHG intensity was plotted against the applied voltage to give a hysteresis loop (Figure S3). The SHG intensity considerably changed at ±18 V, from which the E_c was calculated to be 3.6 V μm^{-1}. This E_c value was smaller than that of (*S*)-**1** (E_c = 4.12 V μm^{-1}),[31] and the small E_c is a desirable feature for achieving ferroelectrics with low energy consumption. Achievement of the low E_c value suggests that the helical column of *rac*-**1** includes several stereoisomers, which weakens the intracolumnar interactions.

Circular Dichroism Experiments of *rac*-1. To investigate the chiral induction in *rac*-**1**, the circular dichroism (CD) spectra of *rac*-**1** were obtained. A chloroform solution of *rac*-**1** (concentration: 3.5 mM) was added dropwise onto a quartz plate and spin-coated to produce a thin film on the quartz plate (film thickness: approximately 4 μm) at room temperature. In each CD measurement, 12 CD spectra were collected by rotating the sample by 30° around the center of the incident light, and then after turning over, 12 more CD spectra were collected in the same way. The resulting 24 CD signals obtained were averaged to minimize the effects of linear birefringence and linear dichroism. The CD spectrum of the thin film, measured at room temperature using incident light through an 8 mm diameter circular slit (Figure 6a), showed a very weak CD signal. In contrast, when a 1 mm diameter circular slit was used instead of the 8 mm diameter slit, as shown in Figure 6b, the intensity and sign of the CD signal measured varied from region to region. A comparison of Figure 6a,b showed that the CD signal obtained with an 8 mm diameter slit was the result of the many CD signals of smaller areas canceling each other out. This result strongly suggests that stereoisomers in the mixture (*rac*-**1**) were separated into opposite chiral domains by self-sorting because a similar CD observation in chiral self-sorting in hexagonal crystal phases was reported by Roche et al.[38] To demonstrate this hypothesis, we prepared a mixture of (*S*)-**1** and (*R*)-**1** at every 10 ratio from 0:100 to 100:0, placed their thin films (thickness: approximately 3 μm) on a quartz plate, and measured their CD spectra. As shown in Figure 6c,d, the intensity of the CD signals (slit diameter: 8 mm) changed in proportion to the enantiomeric excess. This result indicated that the majority rule[39] did not occur when forming helical columns because the CD signal intensity increased linearly with the ratio. In other words, this result meant that the (*S*)-**1** and (*R*)-**1** molecules were self-sorted and separately formed opposite-handedness helical columns,[40] and the columns with the same helicity were organized in a small domain. The DSC traces of (*S*)-**1**, (*R*)-**1**, (*S*)-**1**/(*R*)-**1** mixture, and *rac*-**1** are shown in Figure S4. Since the N_{Col} phase was not observed in the DSC charts of the (*S*)-**1**/(*R*)-**1** mixture, it is assumed that (*S*)-**1** and (*R*)-**1** are slightly miscible with each other. In addition, it is noteworthy that *rac*-**1** showed a simple DSC chart with two sharp transition peaks, although it is a mixture of many stereoisomers.

The results of the above CD experiments suggest that the chiral stereoisomers in *rac*-**1** are self-sorted to form either left-handed [minus (*M*)] or right-handed [plus (*P*)] helical columns separately, and columns with the same helicity assembled into a chiral domain. However, it is necessary to explain the behavior of molecules with no chirality (or weak chirality), such as molecules with three (*S*)- and three (*R*)-citronellyl groups.

https://doi.org/10.1021/acsomega.1c02534
ACS Omega 2021, 6, 18451−18457

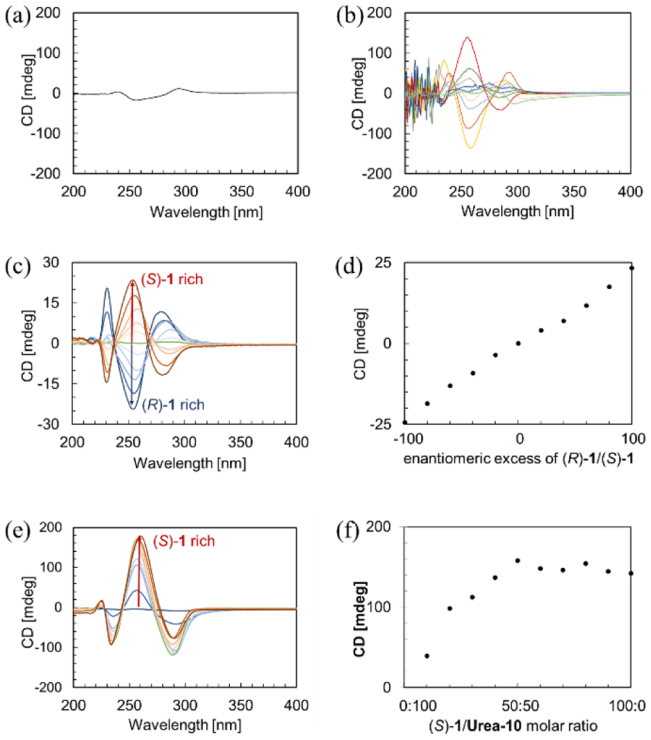

Figure 6. CD measurements of the thin films of Col_r phases: (a) CD spectrum of a *rac*-**1** thin film using an 8 mm diameter slit, (b) CD spectra of several positions of a *rac*-**1** thin film using a 1 mm diameter slit, (c) CD spectra of thin films of (*S*)-**1**/(*R*)-**1** mixtures using an 8 mm diameter slit (red and blue arrows indicate the change in the CD signal with an increasing ratio of (*S*)-**1** and (*R*)-**1**, respectively), (d) plot of the CD signal intensity at 255 nm against ee % of the (*S*)-**1**/(*R*)-**1** mixture, (e) CD spectra of the thin film of (*S*)-**1**/**Urea-10** mixture, using an 8 mm diameter slit (red arrow indicates the change in the CD signal with an increasing ratio of (*S*)-**1**), and (f) plot of the CD signal intensity at 255 nm against the molar ratio of (*S*)-**1**/**Urea-10** mixture.

To determine the behavior of the achiral (or weakly chiral) molecules in the chiral molecules, achiral compound **Urea-10** was mixed with (*S*)-**1**, and DSC and CD measurements of the mixtures were performed. In the DSC experiments (Figure S5), the phase transition temperatures of the mixtures were significantly different from those of pure (*S*)-**1** and **Urea-10**. This result indicated that the two compounds were highly miscible. Figure 6e,f shows the CD signals of the 0:100−100:0 mixture of (*S*)-**1**/**Urea-10** and the plot of their intensity at 255 nm, respectively. The CD signal intensities of the (*S*)-**1**/**Urea-10** mixtures at greater than 50% were almost the same as that of pure (*S*)-**1**. This result suggests that the (*M*)-helical structures generated by the chiral molecules [(*S*)-**1**] were mostly maintained despite the introduction of a small amount of the achiral molecules (**Urea-10**), and these **Urea-10** molecules were incorporated into the (*M*)-helical columns. This result showed contrast to the plot of the CD signal intensities of the (*S*)-**1**/(*R*)-**1** mixtures, as shown in Figure 6d, in which the CD intensities were changed linearly against the ee %.

Estimation of the Packing of Helical Columns from the Electron Density Map. The resolution of the (*M*)- and (*P*)-helical columns to the chiral domains are explained by the chiral selective packing of the columns in the Col_r phase of *rac*-**1**. Although the XRD profile of *rac*-**1** in the Col_r phase did not show any peaks based on the helical structure due to the rather low symmetry of the helicity, our previous study clarified that (*S*)-**1** molecules stack in 30° increments to form an (*M*)-helical column structure.[31] Accordingly, it is assumed that (*R*)-**1** molecules stack to form the mirror image, (*P*)-helical column structure. Figure 7a shows the molecular model of (*S*)-**1**.

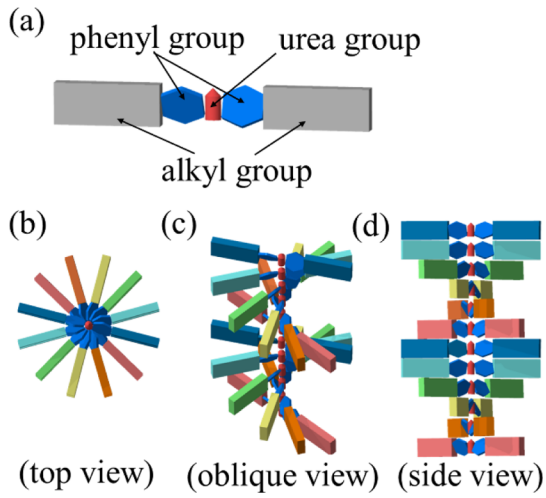

Figure 7. Schematic representation of the (*M*)-helical column of **1**: (a) molecule **1**, (b) top, (c) oblique, and (d) side views of the column. The alkyl chain parts directing the same direction are colorized in the same color (red, orange, yellow, green, light blue, or dark blue).

Figure 7b−d shows the top, oblique, and side views of the (*M*)-helical column, and the alkyl chain parts directing the same direction are colorized in the same color (red, orange, yellow, green, light blue, or dark blue) for clarity. As shown in Figure 8a,b, in the Col_r phase, it is suggested that the alkyl parts of the neighboring two columns interdigitate in the *b*-axis direction. As shown in Figure 8c, the four (*M*)-helical column models are set on the electron density map of *rac*-**1**, and the models fit on the electron density map. Furthermore, since a slight interdigitation occurs even in the *a*-axis direction, it is expected that packing of the columns with the same helicity is prioritized while synchronizing the helical periodicity because of steric interactions. Therefore, the (*M*)-helical columns aggregate to form a chiral domain consisting of only (*M*)-helical columns, while the (*P*)-helical columns form a chiral domain consisting of only (*P*)-helical columns. Furthermore, the non-chiral (or weak chiral) molecules are inserted in either the (*P*)- or (*M*)-helical columns. Thus, only one type of XRD pattern is observed in the Col_r phase of *rac*-**1**.

In the case of (*S*)-**1**, the formation of a helical column played an important role in enhancing the intracolumnar interactions, which were assumed to be enough to maintain the polar columnar structure.[31] As the chiral domains generated in *rac*-**1** are similar to those of (*S*)-**1** or (*R*)-**1**, *rac*-**1** showed an AP-FCLC phase as well as enantiomerically pure (*S*)-**1**.

CONCLUSIONS

In this study, it was clarified that compound *rac*-**1**, which is a mixture of stereoisomers, is self-sorted to form (*M*)- and (*P*)-helical columns, and the columns with the same helicity were adjacent to each other as the chiral domain grew. In this way, *rac*-**1** achieved the same level of ferroelectricity as chiral (*S*)-**1** and (*R*)-**1**. The chiral self-sorting occurred in these simple

https://doi.org/10.1021/acsomega.1c02534
ACS Omega 2021, 6, 18451−18457

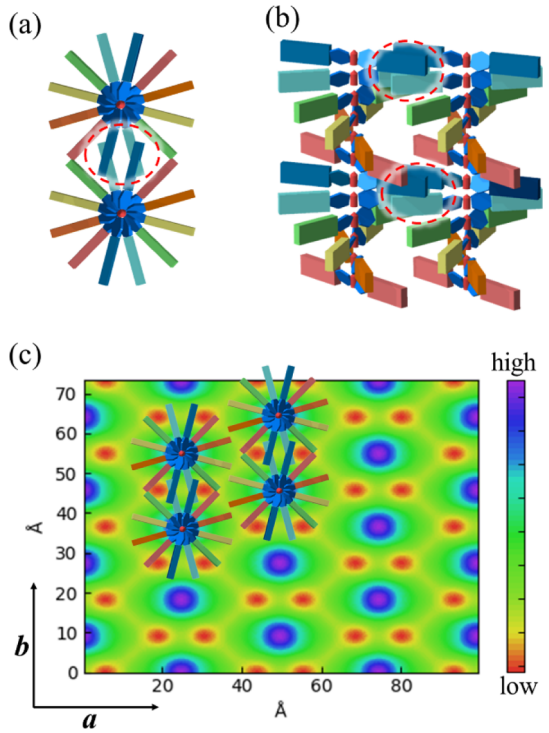

Figure 8. Models for adjacent (*M*)-helical columns in the Col_r phase of (*S*)-**1** and the electron density map of *rac*-**1**: (a) top and (b) side views of the adjacent (*M*)-helical columns (dashed red circles show the intercolumnar interdigitation between alkyl parts in the *b*-axis direction), and (c) the four (*M*)-helical column models set on the electron density map of *rac*-**1** (the color bar indicates the relative electron density obtained from its XRD peak intensities). The arrows *a* and *b* indicate the *a*-axis and *b*-axis directions of the unit lattice.

molecules was surprising, in that 21 kinds of diastereomeric molecules recognized their structural similarities to each other, and that the molecules with similar stereochemistry gathered to generate a chiral column. Furthermore, it was suggested that achiral molecules were included in the chiral helical columns. Thus, it was also important that the stereochemistry of each achiral molecule was not strictly distinguished for the column formation in the LC phase.

Since racemic starting materials are cheaper and more easily available than chiral starting materials, the large-scale synthesis of racemic ureas is much easier than that of chiral ureas, allowing research for a variety of future applications.

■ ASSOCIATED CONTENT

Supporting Information

The Supporting Information is available free of charge at https://pubs.acs.org/doi/10.1021/acsomega.1c02534.

Synthetic procedures and spectral data of *rac*-**1**, (*S*)-**1**, and (*R*)-**1**; reconstruction of relative electron density map of *rac*-**1**; POM images of *rac*-**1** in the Col_h phase; hysteresis loop of *rac*-**1** obtained by the interferometry experiment; DSC traces of (*S*)-**1** and (*R*)-**1**; 1:1 mixture of (*S*)-**1** and (*R*)-**1**, *rac*-**1**; and 80:20 mixture of (*S*)-**1** and **Urea-10**, and **Urea-10** (PDF)

■ AUTHOR INFORMATION

Corresponding Author

Keiki Kishikawa − *Department of Applied Chemistry and Biotechnology, Graduate School of Engineering and Molecular Chirality Research Center, Chiba University, Chiba 263-8522, Japan;* orcid.org/0000-0002-7539-568X; Phone: +81-43-290-3238; Email: kishikawa@faculty.chiba-u.jp

Authors

Miyu Moriya − *Department of Applied Chemistry and Biotechnology, Graduate School of Science and Engineering, Chiba University, Chiba 263-8522, Japan*

Michinari Kohri − *Department of Applied Chemistry and Biotechnology, Graduate School of Engineering and Molecular Chirality Research Center, Chiba University, Chiba 263-8522, Japan;* orcid.org/0000-0003-1118-5568

Complete contact information is available at: https://pubs.acs.org/10.1021/acsomega.1c02534

Author Contributions

The authors contributed equally to this work.

Notes

The authors declare no competing financial interest.

■ ACKNOWLEDGMENTS

This work was supported by the JSPS KAKENHI grant numbers 17H03035 and 20H02809. K.K. thank Dr. H. Ozaki who saved his life with a brain hemorrhage operation 7 years ago. A computing server at the Institute of Management and Information Technologies, Chiba University, was used for computational simulation. We especially thank Dr. T. Ohkubo for his support in setting the calculation conditions.

■ REFERENCES

(1) Kishikawa, K.; Nakahara, S.; Nishikawa, Y.; Kohmoto, S.; Yamamoto, M. A ferroelectrically switchable columnar liquid crystal phase with achiral molecules: superstructures and properties of liquid crystalline ureas. *J. Am. Chem. Soc.* **2005**, *127*, 2565−2571.

(2) Kishikawa, K.; Nakahara, S.; Nishikawa, Y.; Natsukawa, M.; Kohmoto, S. Ferroelectrically switchable columnar liquid crystalline ureas. *Mol. Cryst. Liq. Cryst.* **2009**, *498*, 11−18.

(3) Araoka, F.; Masuko, S.; Kogure, A.; Miyajima, D.; Aida, T.; Takezoe, H. High-optical-quality ferroelectric film wet-processed from a ferroelectric columnar liquid crystal as observed by nonlinear-optical microscopy. *Adv. Mater.* **2013**, *25*, 4014−4017.

(4) Miyajima, D.; Araoka, F.; Takezoe, H.; Kim, J.; Kato, K.; Takata, M.; Aida, T. Ferroelectric Columnar Liquid Crystal Featuring Confined Polar Groups Within Core-Shell Architecture. *Science* **2012**, *336*, 209−213.

(5) Takezoe, H.; Araoka, F. Polar columnar liquid crystals. *Liq. Cryst.* **2014**, *41*, 393−401.

(6) Takezoe, H. Polar liquid crystals - ferro, antiferro, banana, and columnar. *Mol. Cryst. Liq. Cryst.* **2017**, *646*, 46−65.

(7) Nguyen, M. L.; Cho, B. K. Ferroelectrically Switchable Axial Polarization in Columnar Liquid Crystalline Phases. *Chem.—Eur. J.* **2020**, *26*, 6964−6975.

(8) Jakli, A.; Saupe, A.; Scherowsky, G.; Chen, X. H. Indication of ferroelectricity in columnar mesophases of pyramidic molecules. *Liq. Cryst.* **1997**, *22*, 309−316.

(9) Gorecka, E.; Pociecha, D.; Mieczkowski, J.; Matraszek, J.; Guillon, D.; Donnio, B. Axially Polar Columnar Phase Made of Polycatenar Bent-Shaped Molecules. *J. Am. Chem. Soc.* **2004**, *126*, 15946−15947.

(10) Kardas, D.; Prehm, M.; Baumeister, U.; Pociecha, D.; Reddy, R. A.; Mehl, G. H.; Tschierske, C. End functionalized liquid crystalline bent-core molecules and first DAB derived dendrimers with banana shaped mesogenic units. *J. Mater. Chem.* **2005**, *15*, 1722−1733.
(11) Amaranatha Reddy, R.; Baumeister, U.; Chao, J. L.; Kresse, H.; Tschierske, C. Silylated bent-core molecules: the influence of the direction of the carboxyl connecting groups on the mesophase behavior. *Soft Matter* **2010**, *6*, 3883−3897.
(12) Li, X.; Zhan, M.-s.; Wang, K. A hexagonal columnar phase formed in lateral fluorinated bent-shaped molecules based on a 1,7-naphthalene central core. *New J. Chem.* **2012**, *36*, 1133−1136.
(13) Deepa, G. B.; Radhika, S.; Sadashiva, B. K.; Pratibha, R. Electric-field-induced switchable dark conglomerate phases in a bent-core liquid crystal exhibiting reverse columnar phases. *Phys. Rev. E* **2013**, *87*, 062508.
(14) Yoshio, M.; Konishi, R.; Sakamoto, T.; Kato, T. Bi-sphenylsulfone-based molecular assemblies: polar columnar liquid crystals aligned in electric fields and fibrous aggregates in organic solvents. *New J. Chem.* **2013**, *37*, 143−147.
(15) Yelamaggad, C. V.; Shanker, G.; Rao, R. V. R.; Rao, D. S. S.; Prasad, S. K.; Babu, V. V. S. Supramolecular helical fluid columns from self-assembly of homomeric dipeptides. *Chem.—Eur. J.* **2008**, *14*, 10462−10471.
(16) Fitié, C. F. C.; Roelofs, W. S. C.; Kemerink, M.; Sijbesma, R. P. Remnant Polarization in Thin Films from a Columnar Liquid Crystal. *J. Am. Chem. Soc.* **2010**, *132*, 6892−6893.
(17) Shishido, Y.; Anetai, H.; Takeda, T.; Hoshino, N.; Noro, S.-i.; Nakamura, T.; Akutagawa, T. Molecular Assembly and Ferroelectric Response of Benzenecarboxamides Bearing Multiple -$CONHC_{14}H_{29}$ Chains. *J. Phys. Chem. C* **2014**, *118*, 21204−21214.
(18) Anetai, H.; Wada, Y.; Takeda, T.; Hoshino, N.; Yamamoto, S.; Mitsuishi, M.; Takenobu, T.; Akutagawa, T. Fluorescent Ferroelectrics of Hydrogen-Bonded Pyrene Derivatives. *J. Phys. Chem. Lett.* **2015**, *6*, 1813−1818.
(19) Meng, X.; Gorbunov, A. V.; Christian Roelofs, W. S.; Meskers, S. C. J.; Janssen, R. A. J.; Kemerink, M.; Sijbesma, R. P. Ferroelectric switching and electrochemistry of pyrrole substituted trialkylbenzene-1,3,5-tricarboxamides. *J. Polym. Sci., Part B: Polym. Phys.* **2017**, *55*, 673−683.
(20) Casellas, N. M.; Urbanaviciute, I.; Cornelissen, T. D.; Berrocal, J. A.; Torres, T.; Kemerink, M.; García-Iglesias, M. Resistive switching in organic supramolecular semiconducting ferroelectric. *Chem. Commun.* **2019**, *55*, 8828−8831.
(21) Urbanaviciute, I.; Bhattacharjee, S.; Biler, M.; Lugger, J. A. M.; Cornelissen, T. D.; Norman, P.; Linares, M.; Sijbesma, R. P.; Kemerink, M. Suppressing depolarization by tail substitution in an organic supramolecular ferroelectric. *Phys. Chem. Chem. Phys.* **2019**, *21*, 2069−2079.
(22) Anetai, H.; Sambe, K.; Takeda, T.; Hoshino, N.; Akutagawa, T. Nanoscale effects in one-dimensional columnar supramolecular ferroelectrics. *Chem.—Eur. J.* **2019**, *25*, 11233−11239.
(23) Wu, J.; Takeda, T.; Hoshino, N.; Akutagawa, T. Ferroelectric low-voltage ON/OFF switching of chiral benzene-1,3,5-tricarboxamide derivative. *J. Mater. Chem. C* **2020**, *8*, 10283−10289.
(24) Wu, J.; Takeda, T.; Hoshino, N.; Akutagawa, T. Mixed Columnar Assembly of Ferroelectric and Antiferroelectric Benzene Derivatives Bearing Multiple -$CONHC_{14}H_{29}$ Chains. *J. Phys. Chem. B* **2020**, *124*, 7067−7074.
(25) Miyajima, D.; Araoka, F.; Takezoe, H.; Kim, J.; Kato, K.; Takata, M.; Aida, T. Electric-Field-Responsive Handle for Large-Area Orientation of Discotic Liquid-Crystalline Molecules in Millimeter-Thick Films. *Angew. Chem., Int. Ed.* **2011**, *50*, 7865−7869.
(26) Miyajima, D.; Araoka, F.; Takezoe, H.; Kim, J.; Kato, K.; Takata, M.; Aida, T. Columnar Liquid Crystal with a Spontaneous Polarization along the Columnar Axis. *J. Am. Chem. Soc.* **2010**, *132*, 8530−8531.
(27) Miyajima, D.; Tashiro, K.; Araoka, F.; Takezoe, H.; Kim, J.; Kato, K.; Takata, M.; Aida, T. Liquid Crystalline Corannulene Responsive to Electric Field. *J. Am. Chem. Soc.* **2009**, *131*, 44−45.
(28) Sato, K.; Itoh, Y.; Aida, T. Columnarly Assembled Liquid-Crystalline Peptidic Macrocycles Unidirectionally Orientable over a Large Area by an Electric Field. *J. Am. Chem. Soc.* **2011**, *133*, 13767−13769.
(29) Kishikawa, K.; Nakahara, S.; Natsukawa, M.; Suzuki, K.; Kohmoto, S. Relation between the Spontaneous Polarization and Alkyl Chain Length in Ferroelectric Switching of Columnar Liquid-Crystalline Ureas. *Mol. Cryst. Liq. Cryst.* **2010**, *516*, 107−113.
(30) Akiyama, A.; Kohri, M.; Kishikawa, K. A Low-temperature Axially Polar Ferroelectric Columnar Liquid Crystal Compound Possessing Branched Alkyl Chains. *Chem. Lett.* **2020**, *49*, 768−770.
(31) Akiyama, A.; Jido, K.; Kohri, M.; Taniguchi, T.; Kishikawa, K. Generation of Axially Polar Ferroelectricity in a Columnar Liquid Crystal Phase by Introducing Chirality. *Adv. Electron. Mater.* **2020**, *6*, 2000201.
(32) Nguyen, M. L.; Byun, J.; Kim, S.; Hyun, J. W.; Hur, K.; Shin, T. J.; Cho, B. K. Ferroelectrically Switching Helical Columnar Assembly Comprising Cisoid Conformers of a 1,2,3-Triazole-based Liquid Crystal. *Angew. Chem., Int. Ed.* **2019**, *58*, 2749−2753.
(33) García-Iglesias, M.; de Waal, B. F. M.; Gorbunov, A. V.; Palmans, A. R. A.; Kemerink, M.; Meijer, E. W. A Versatile Method for the Preparation of Ferroelectric Supramolecular Materials via Radical End-Functionalization of Vinylidene Fluoride Oligomers. *J. Am. Chem. Soc.* **2016**, *138*, 6217−6223.
(34) Fitié, C. F. C.; Roelofs, W. S. C.; Magusin, P. C. M. M.; Wübbenhorst, M.; Kemerink, M.; Sijbesma, R. P. Polar Switching in Trialkylbenzene-1,3,5-tricarboxamides. *J. Phys. Chem. B* **2012**, *116*, 3928−3937.
(35) Gorbunov, A. V.; Putzeys, T.; Urbanavičiūtė, I.; Janssen, R. A. J.; Wübbenhorst, M.; Sijbesma, R. P.; Kemerink, M. True ferroelectric switching in thin films of trialkylbenzene-1,3,5-tricarboxamide (BTA). *Phys. Chem. Chem. Phys.* **2016**, *18*, 23663−23672.
(36) Gorbunov, A. V.; Garcia Iglesias, M.; Guilleme, J.; Cornelissen, T. D.; Roelofs, W. S. C.; Torres, T.; González-Rodríguez, D.; Meijer, E. W.; Kemerink, M. Ferroelectric self-assembled molecular materials showing both rectifying and switchable conductivity. *Sci. Adv.* **2017**, *3*, No. e1701017.
(37) Okada, Y.; Matsumoto, S.; Takanishi, Y.; Ishikawa, K.; Nakahara, S.; Kishikawa, K.; Takezoe, H. Polarization switching in a columnar liquid crystalline urea as studied by optical second-harmonic generation interferometry. *Phys. Rev. E* **2005**, *72*, 020701.
(38) Roche, C.; Sun, H.-J.; Prendergast, M. E.; Leowanawat, P.; Partridge, B. E.; Heiney, P. A.; Araoka, F.; Graf, R.; Spiess, H. W.; Zeng, X.; Ungar, G.; Percec, V. Homochiral Columns Constructed by Chiral Self-Sorting During Supramolecular Helical Organization of Hat-Shaped Molecules. *J. Am. Chem. Soc.* **2014**, *136*, 7169−7185.
(39) Cheon, K. S.; Selinger, J. V.; Green, M. M. Counterintuitive influence of microscopic chirality on helical order in polymers. *J. Phys. Org. Chem.* **2004**, *17*, 719−723.
(40) Sato, K.; Itoh, Y.; Aida, T. Homochiral supramolecular polymerization of bowl-shaped chiral macrocycles in solution. *Chem. Sci.* **2014**, *5*, 136−140.

https://doi.org/10.1021/acsomega.1c02534
ACS Omega 2021, 6, 18451−18457